



Nagoya University

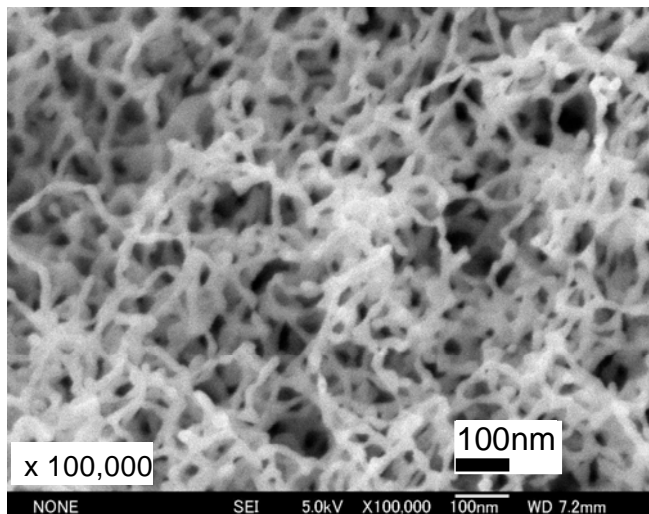
AIT
AICHI
INSTITUTE OF
TECHNOLOGY

核融合炉におけるプラズマ対向壁材料としての タングステンの表面特性

高村 秀一¹、宮本 隆徳¹、大野哲靖²

¹愛知工業大学工学部

²名古屋大学大学院工学研究科



Acknowledgement:

Y. Kikuchi (U. Hyogo)
D. Nishijima (UCSD)
S. Kajita (Nagoya U.)
K. Ohya (Tokuhima U.)

ナノ構造を含むタンゲステン材料の表面特性

- (1) ナノ構造表面の修復
- (2) ナノ構造の冷却効果 (計測: 放射温度計; 熱電対)
- (3) ナノ構造における2次電子放出特性
- (4) ナノ構造のスパッタリング特性
- (5) ナノ構造におけるクラッキング耐性
- (6) ナノ構造におけるアーキング誘発性
- (7) タンゲステン表面からの放射特性 (Total Emissivity を用いて)

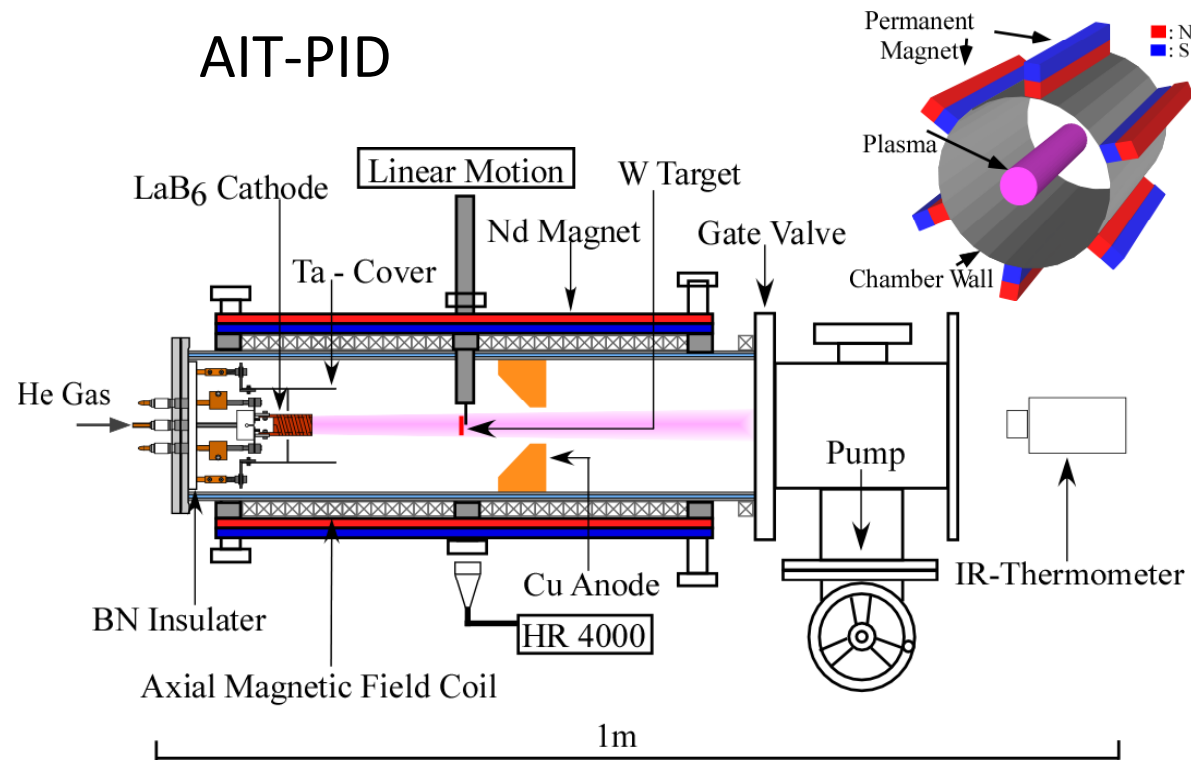


Objective: Characterization for Wall of Fusion Reactor

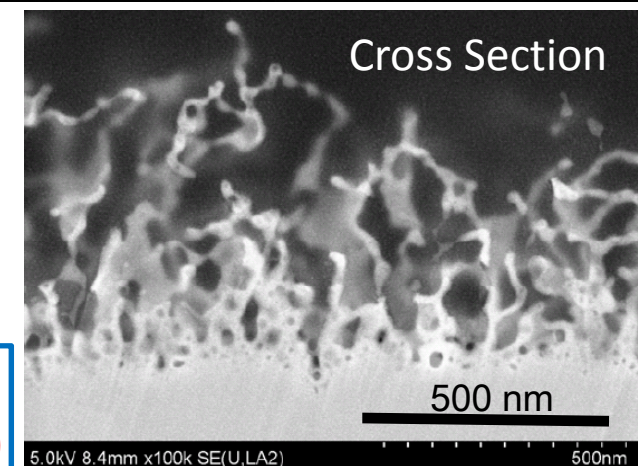
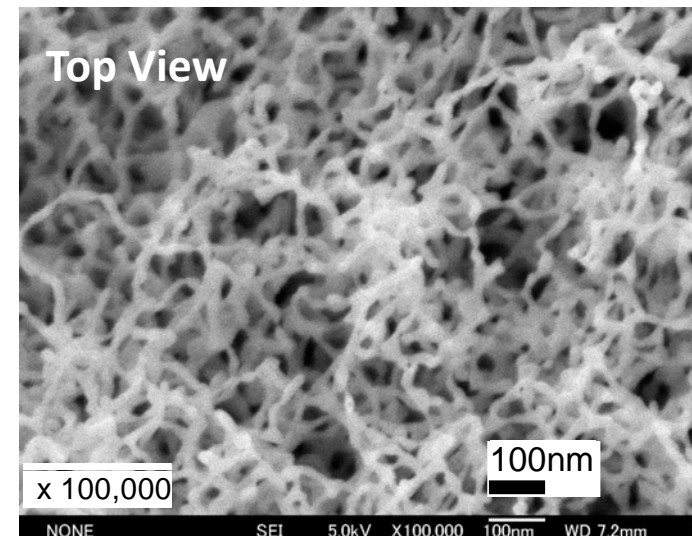
Device Specification of AIT-PID

(Aichi Institute of Technology - Plasma Irradiation Device)

AIT-PID



Plasma Density $> 1 \times 10^{18} \text{ m}^{-3}$; Ion Flux : $1 \times 10^{22} \text{ m}^{-2}\text{s}^{-1}$
Electron Temperature : 4 eV with ~10% Hot component(40 eV)
Deep Floating Voltage : 40 V



Recovery of Tungsten Surface by Plasma Annealing

Recovery may be obtained with some bubbles remained underneath the surface!

S. Takamura and T. Miyamoto :

Plasma Fusion Res. **6** (2010) 005.

Recovered target →

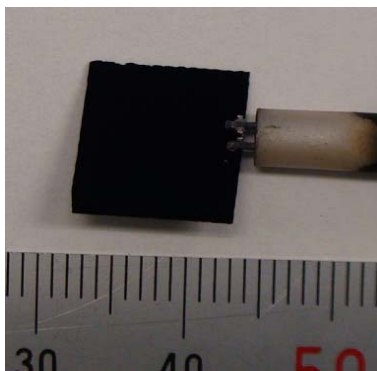
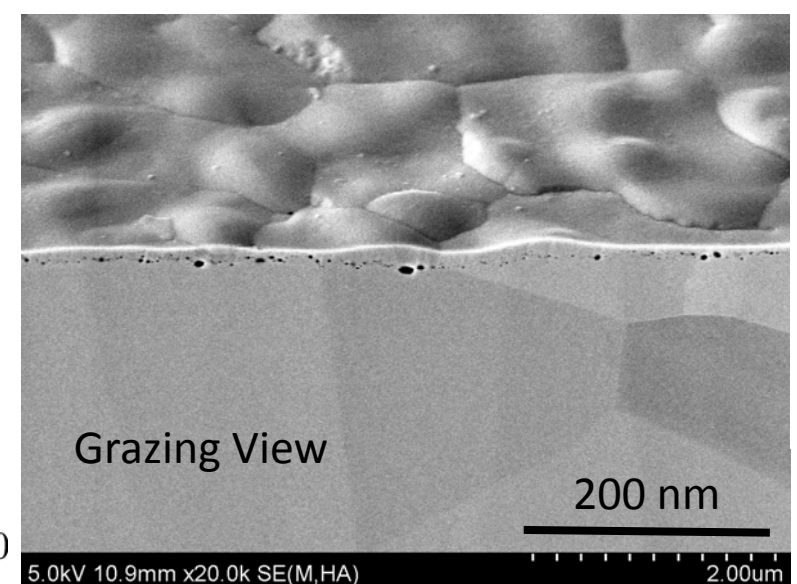
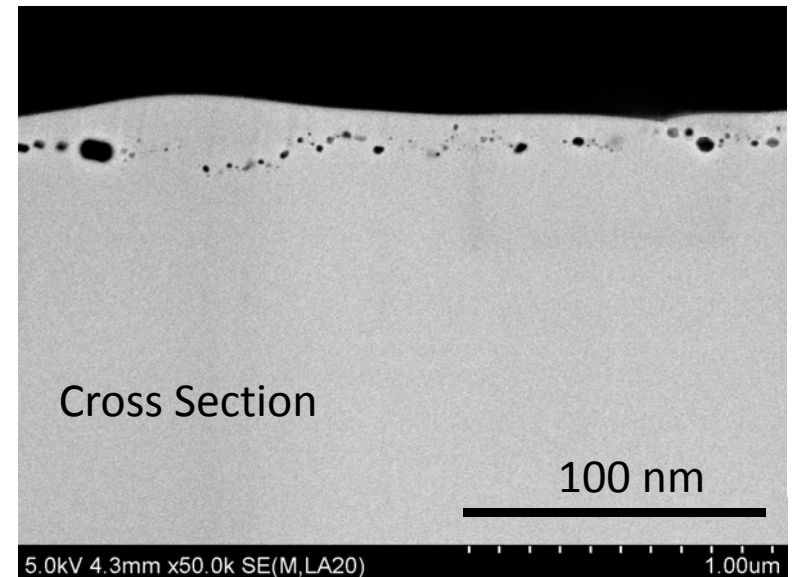
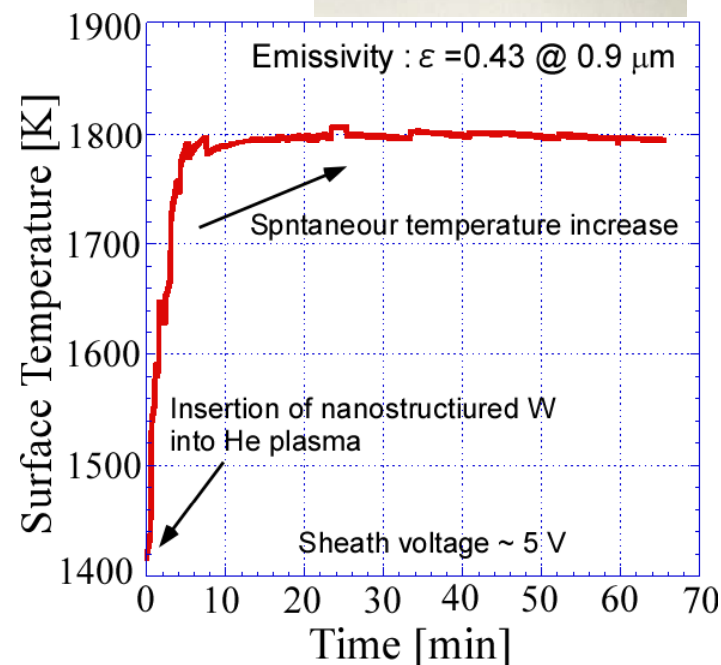


Photo of
nanostructured
tungsten target



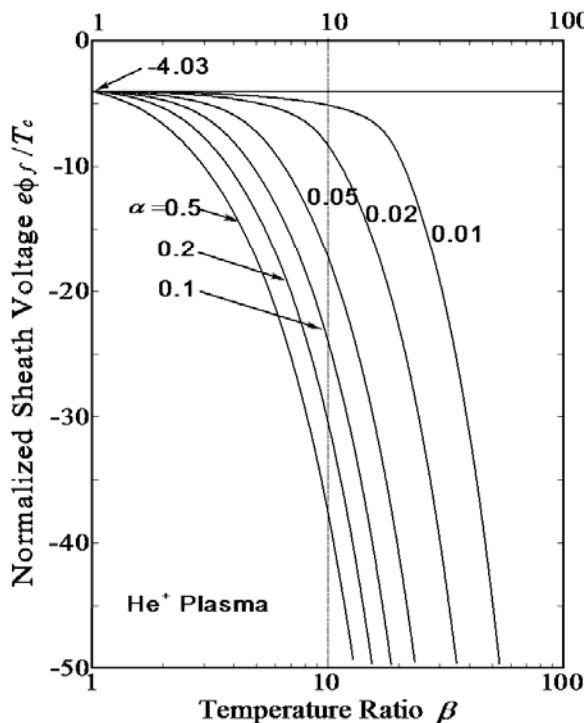
Cooling associated by suppression of SEE

高エネルギー電子成分がプラズマ熱流を高め、
シース電圧を深くしている！

$$\left(1 - \alpha + \frac{\alpha}{\beta}\right)^{-1/2} = \sqrt{\frac{m_i}{2\pi m_e}} \left\{ (1 - \alpha) e^{e\phi_f/T_c} + \alpha \sqrt{\beta} e^{e\phi_f/T_h} \right\}$$

Takizuka's Criterion

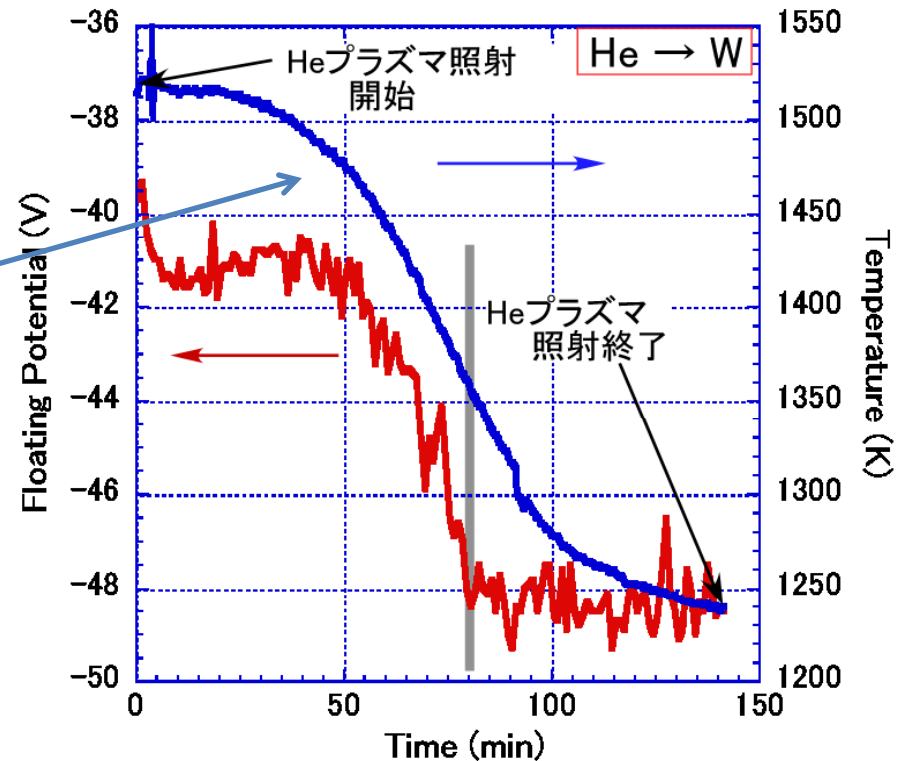
$$\alpha > \beta^{-1/2} \left(\frac{2\pi m_e}{m_i} \right)^{0.5 - \left(\frac{1}{2\beta} \right)} = 0.013 \quad (\beta = 10)$$



放射温度計
による測定
放射率の問題

Sheath voltage = $V_p - V_f = 40\sim50$ V
in stead of $4T_e \sim 16$ V

$$\alpha = n_h/n_c = 8\% \\ \beta = T_h/T_c = 40/4 \text{ eV}$$



タンゲステン板からの電子放出が阻害される？

Favorable Property #1: Surface Cooling

放射入力に比してプラズマ熱負荷が
圧倒的に大きいとすると、

$$P_{\text{plasma}} [\text{W}] = \varepsilon_t(T) \sigma T^4 [\text{K}] S [\text{m}^2]$$

$$T = \left(\frac{P}{\varepsilon_t \sigma S} \right)^{1/4}$$

$\varepsilon_t(T)$: Total Emissivity

σ : Stephan-Boltzmann's
constant

S : Surface area

T : Surface Temperature

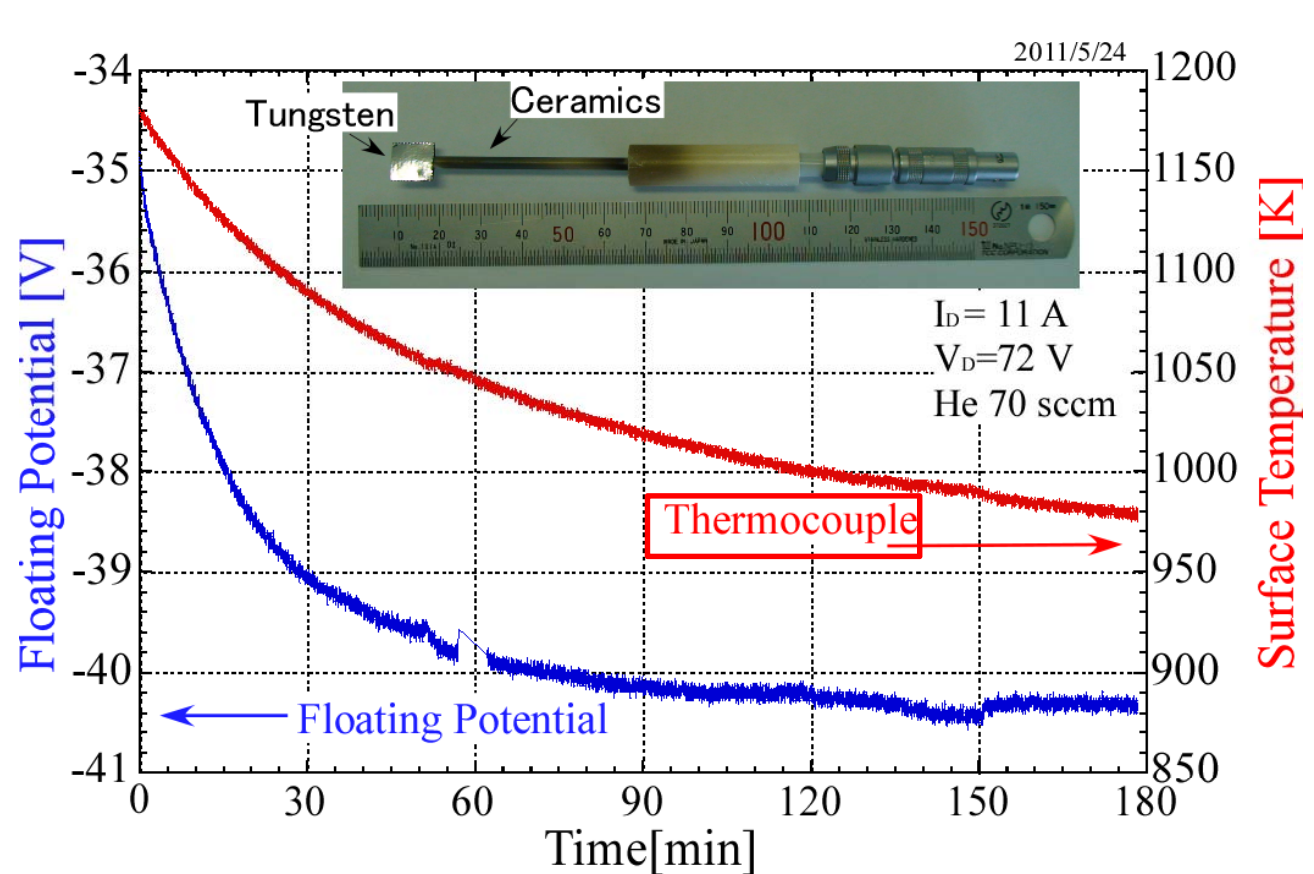
P_{plasma} : Plasma Heat Load

$\varepsilon_t \sim 0.15$

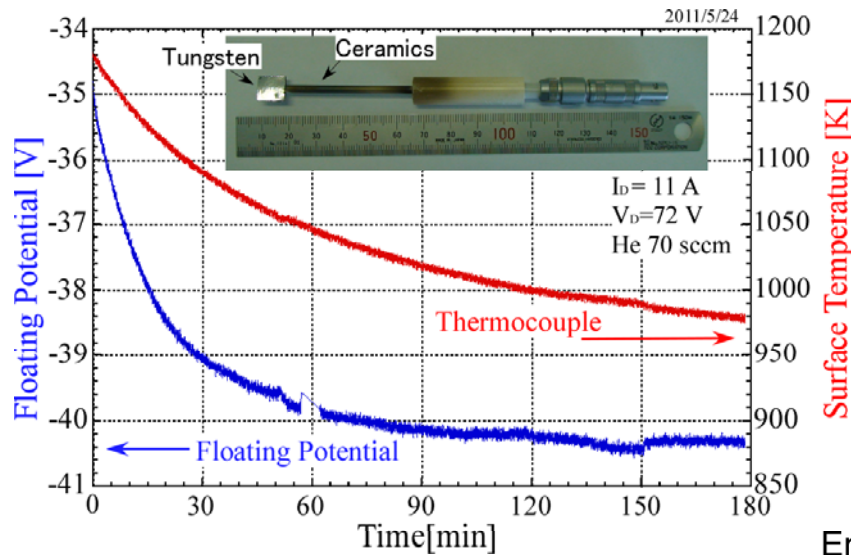
~Black Body
?

Physical Mechanisms for Surface Cooling :

- (1) Increase in Radiation Emissivity (blackening)
- (2) Deepening of Floating Potential



Favorable Property #2: Suppression of SEE



S.Takamura, T. Miyamoto and N. Ohno,
 Plasma Fusion Res. **5** (2010) 039.

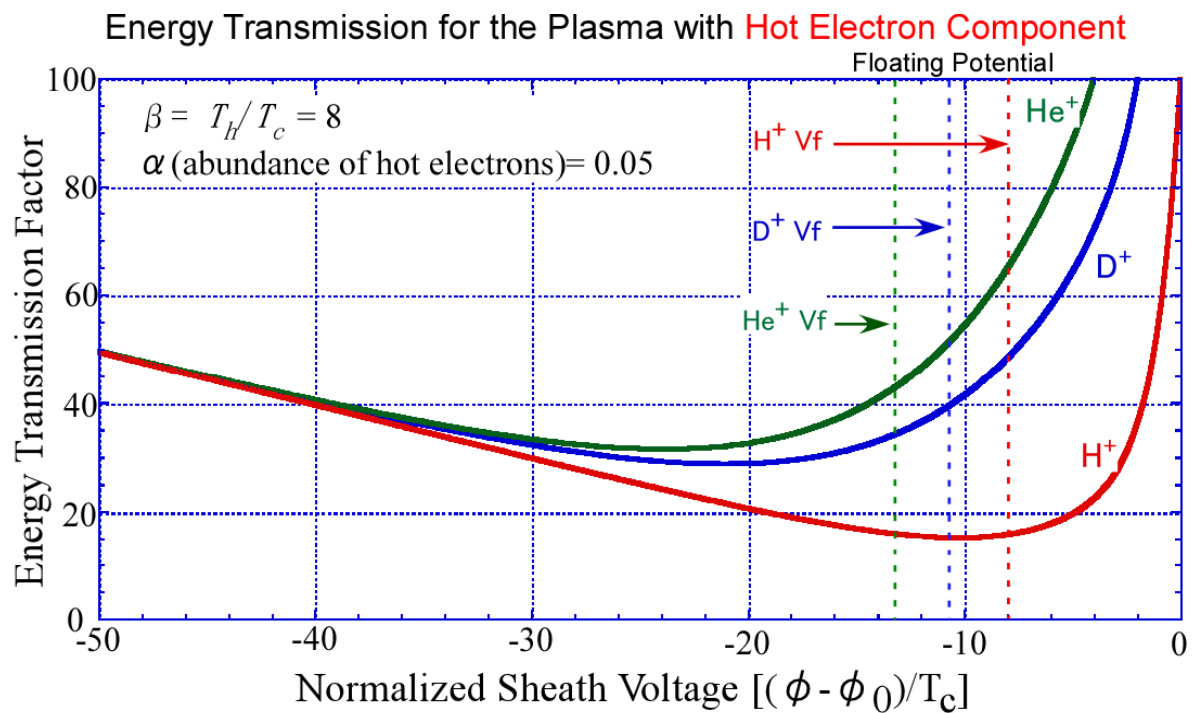
Deepening of floating potential
 gives
 a smaller **energy transmission factor**
 through the sheath.

Why is the floating potential
 deepened?

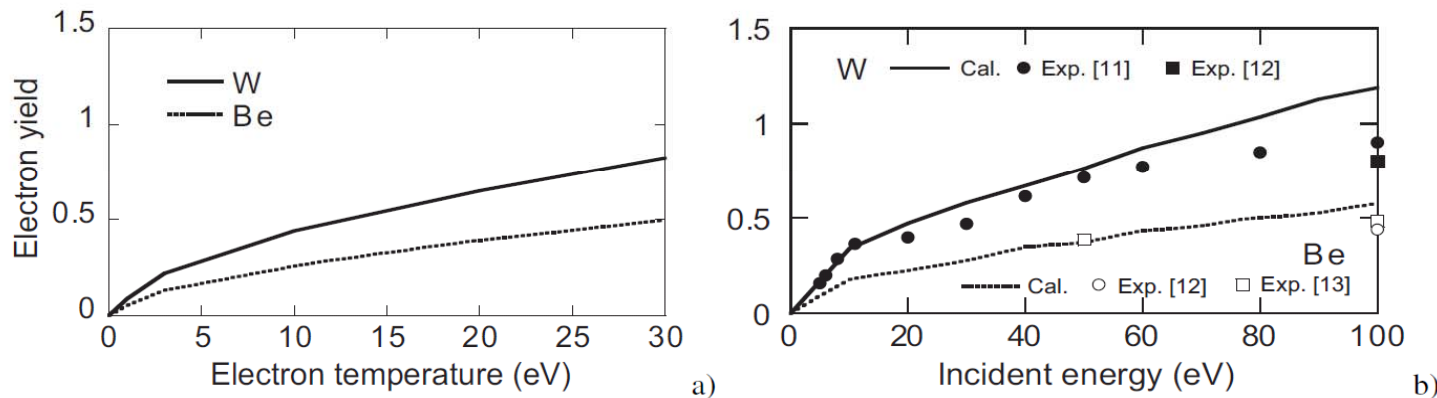


Suppression of SEE ?
 (Secondary Electron Emission)

$$P / (T_e \cdot I_{is})$$



Favorable Property #2: Suppression of SEE (continued)



Tungsten W has
a fairly large SEE !

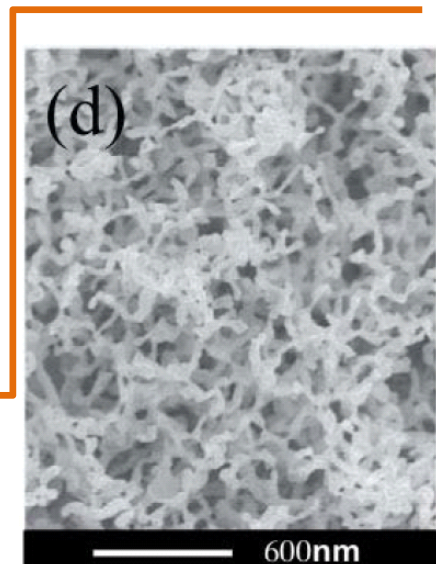


Fig. 2 Electron yield, which includes both BSEs and SEs, as a function of (a) the electron temperature at the angle $\varphi = 0^\circ$ and (b) the electron energy at normal incidence.

K. Imai, K. Ohya, G. Kawamura, and Y. Tomita: Contrib. Plasma Phys. **50** (2010) 458-463.

研究論文

Monte Carlo Approach to Secondary Electron Emission from Rough Surfaces of Beryllium

河田, 大宅

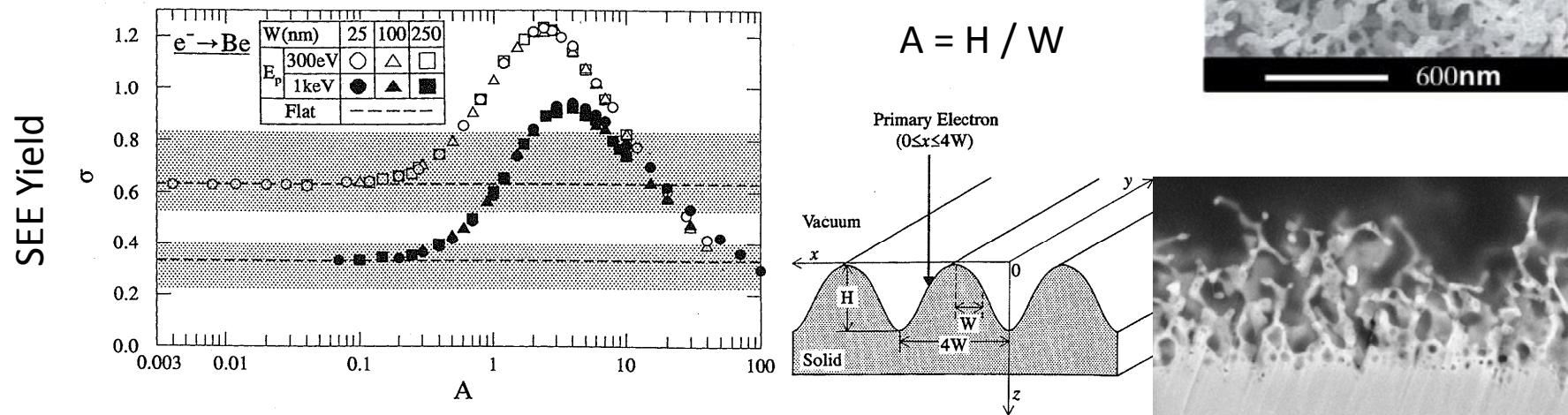


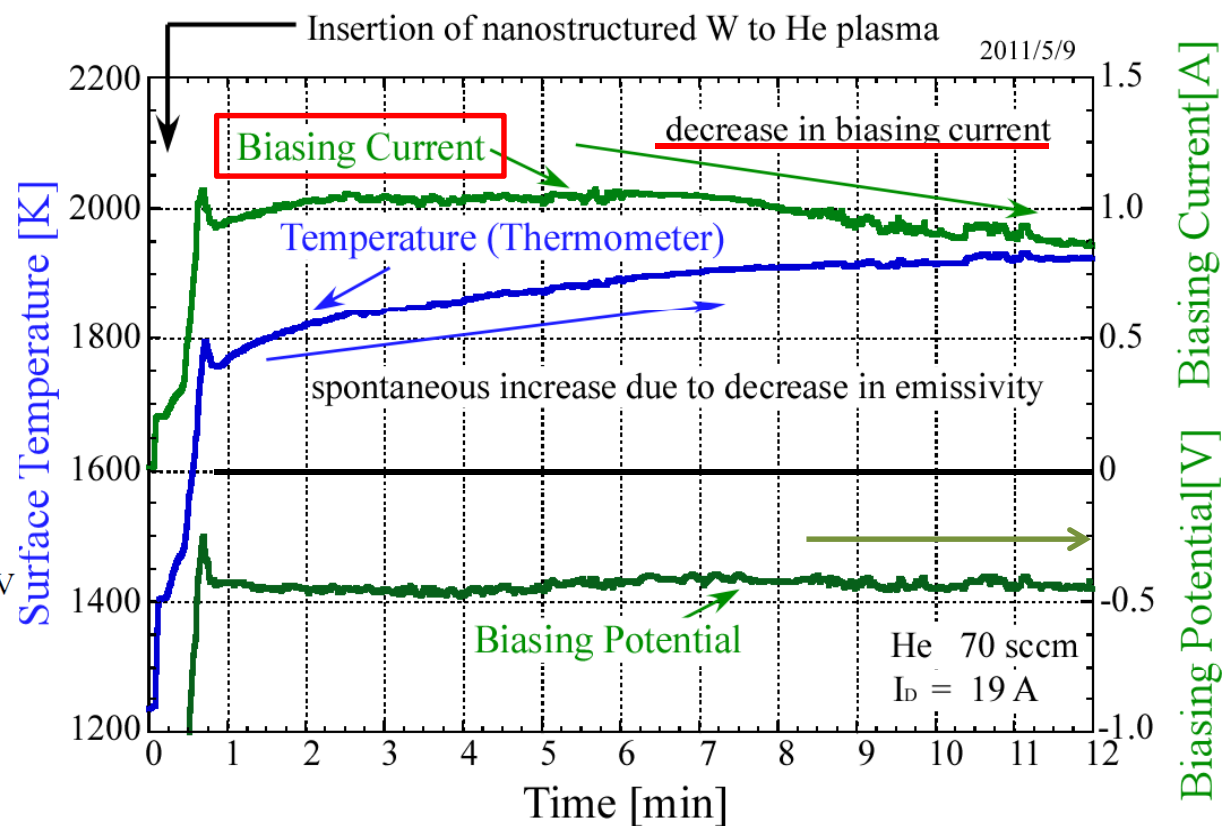
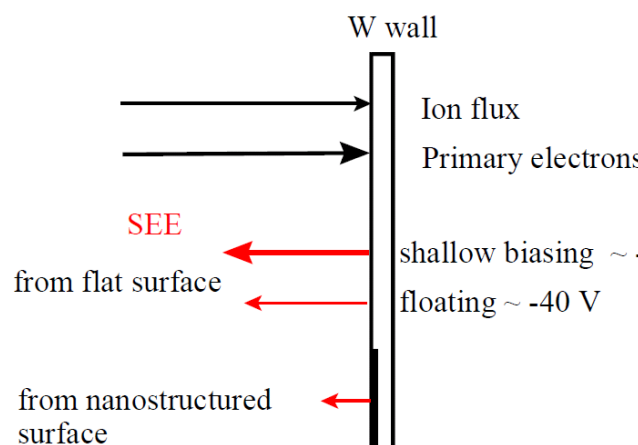
Fig. 3 Variations of the secondary electron yield σ with the ratio $A (= H / W)$ for surface roughness under 300-eV and 1-keV electron bombardments. The data points are calculated by changing the depth H on condition of constant widths W ; the circles, triangles and squares correspond to the width $W = 25, 100$ and 250nm , respectively. The dashed lines are the calculated σ with a flat surface, and the shaded zones represent the amplitude of scatter of data among different experiments [4-7].

J. Kawata and K. Ohya: J. Plasma Fusion Res. **70** (1994) 84.

Favorable Property #2: Suppression of SEE (continued)

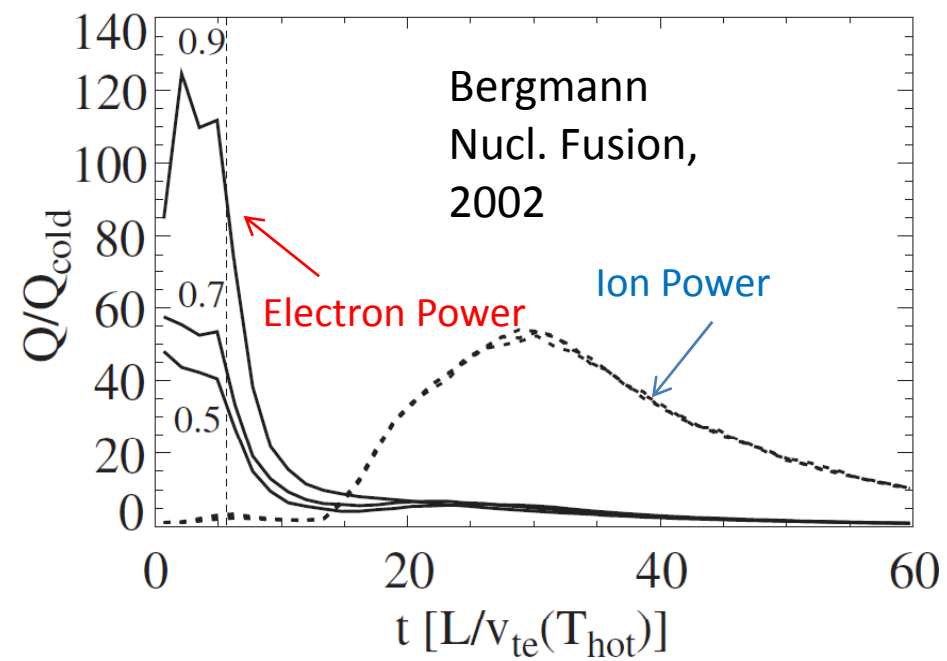
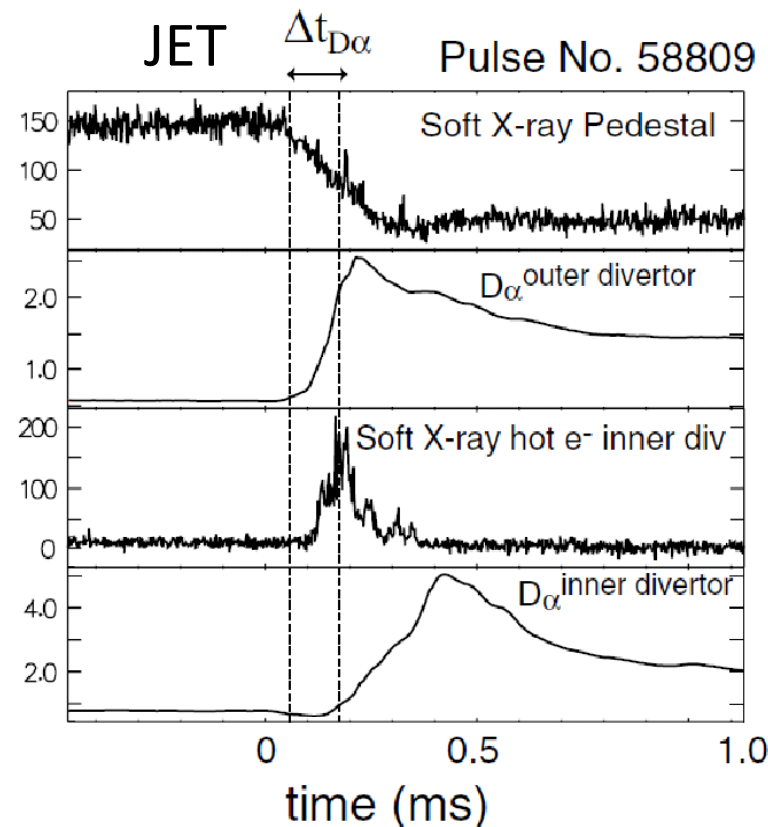
The effect of SEE is demonstrated in a different way . It is a kind of recovery process for a W plate with a black surface by increasing the plasma electron heat flux obtained by approaching the biasing potential to nearly 0 V. The surface temperature increases in time because the nano-fibers on the surface shrink so that the emissivity decreases.

The remarkable phenomenon is a reductions of biasing electron current even under an almost a fixed or even decreasing biasing voltage. It is believed that the reduction of biasing current is caused by a recovery of SEE because the W surface is gradually smoothed in time. The incident energy of hot electrons is larger than that in floating condition.

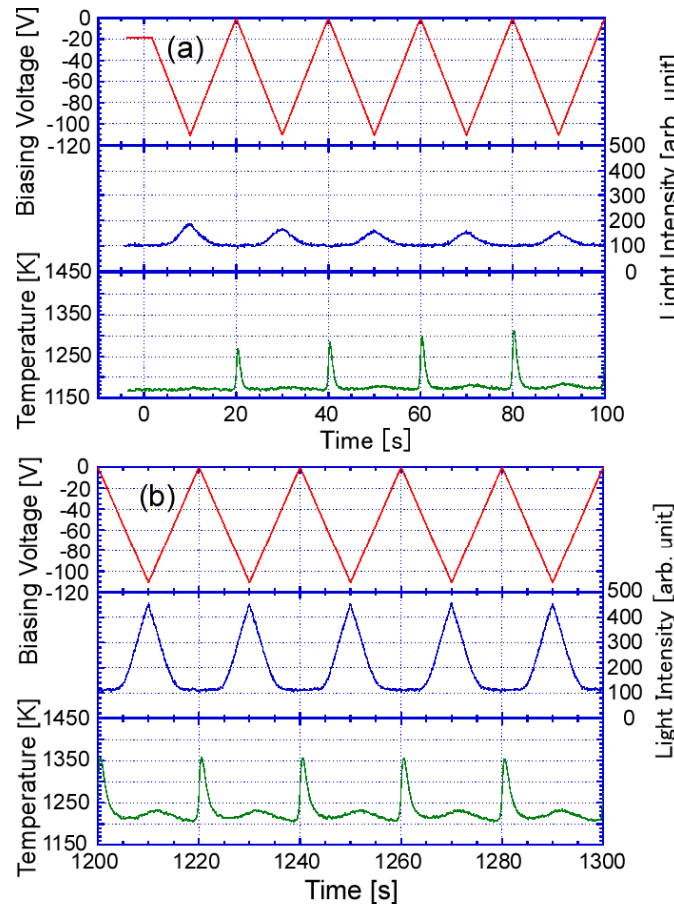


Favorable Property #2: Suppression of SEE (continued)

Suppression of SEE may quench the enormous influx of electron heat load at the leading edge of ELM.



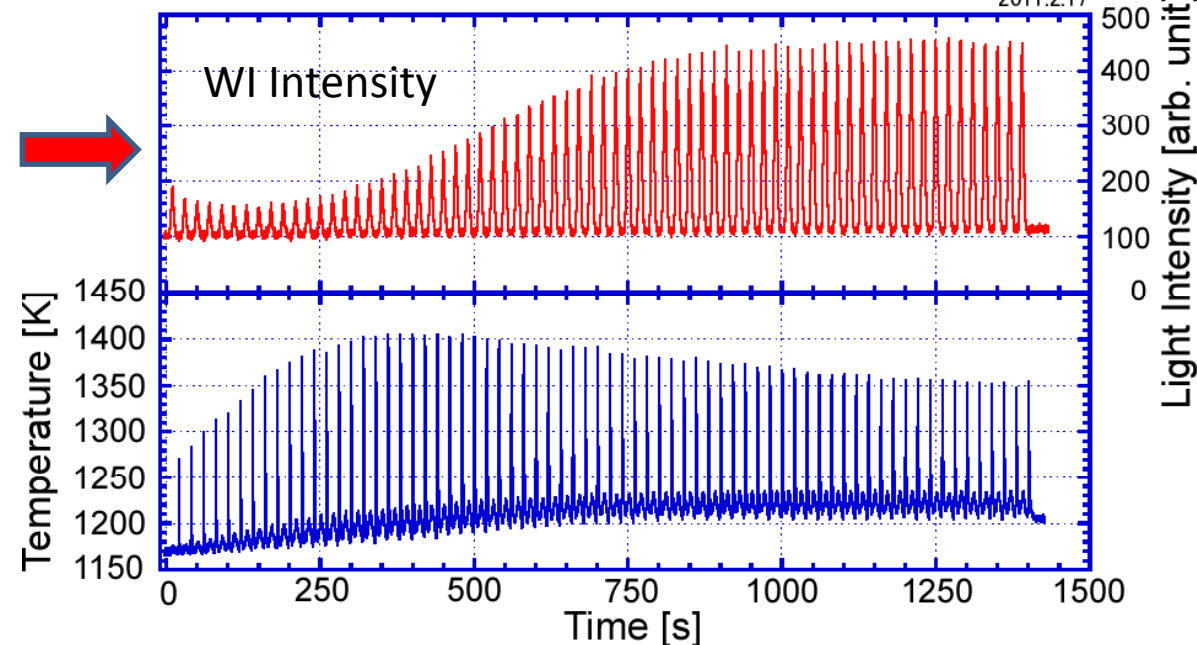
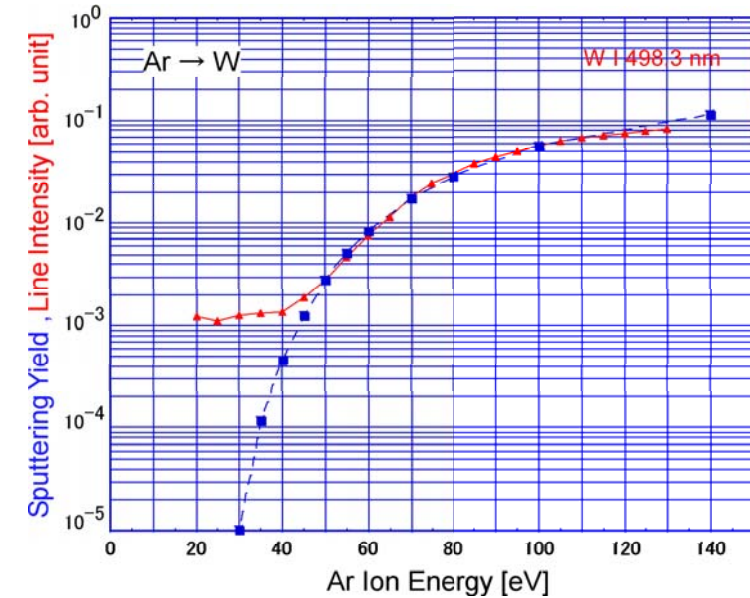
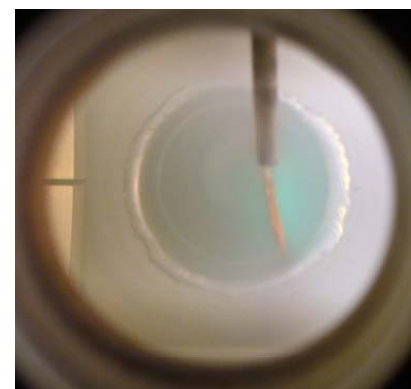
Favorable Property #3: Suppression of Sputtering



Similar behaviors have been already reported :

D. Nishijima et al., 19th PSI Conf. SanDiego California, May 24-28, 2010, O-02, accepted for publication in J. Nucl. Mater.; doi:10.1016/j.jnucmat.2010.12.017.

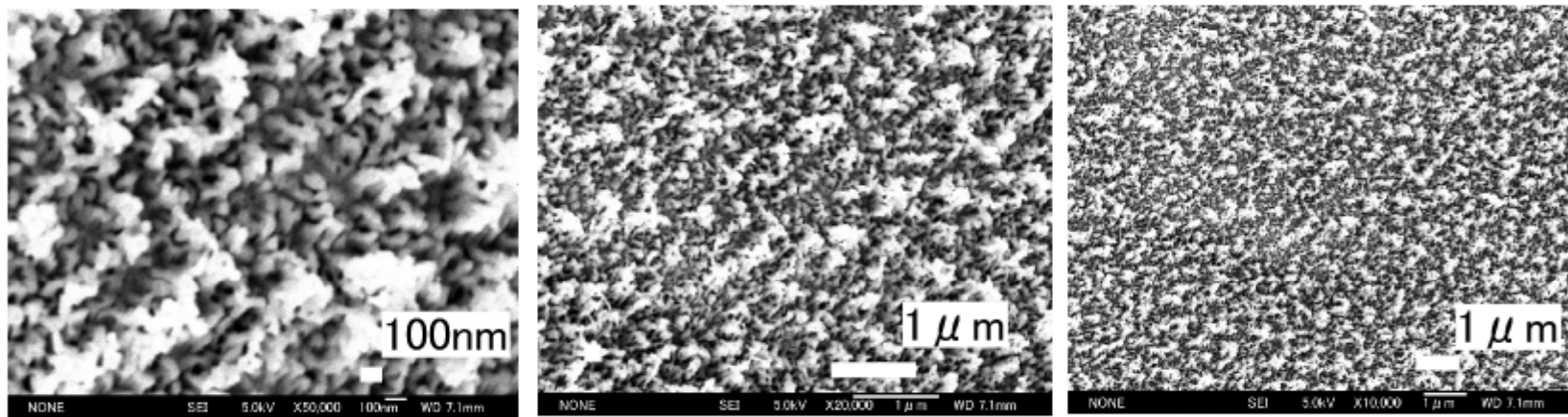
W I 498.2593nm
In Ar Plasma



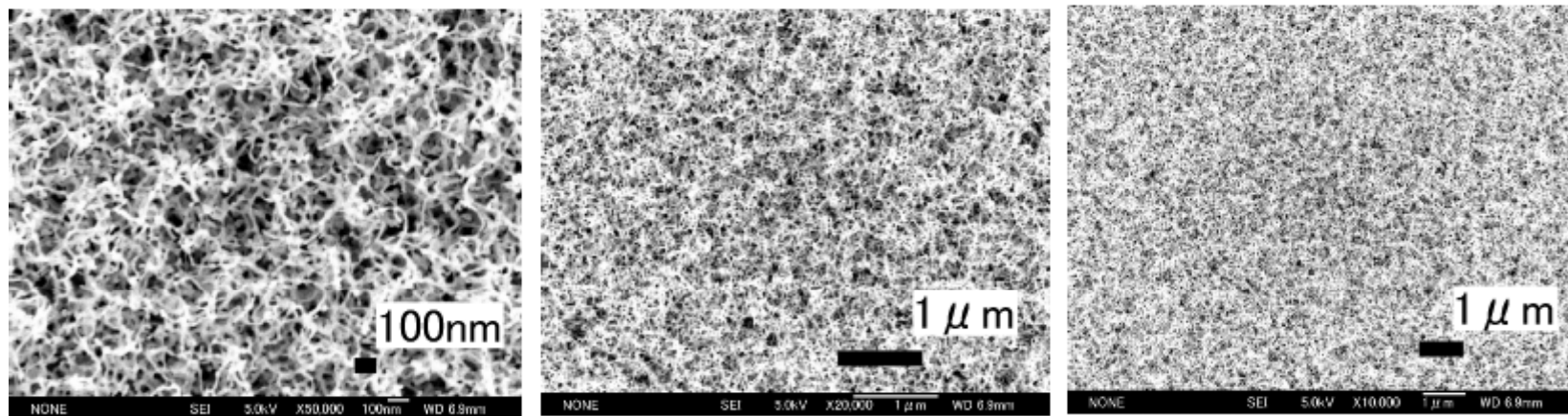
Favorable Property #3: Suppression of Sputtering

Why is there a **minimum** for the sputtering yield ?

SEM Images at the Sputtering Minimum



SEM Images of Nanostructured W without any Sputtering



Favorable Property #4 : Resistance against Cracking

Fiber-form nanostructured surfaces possess a good resistance to surface cracking !

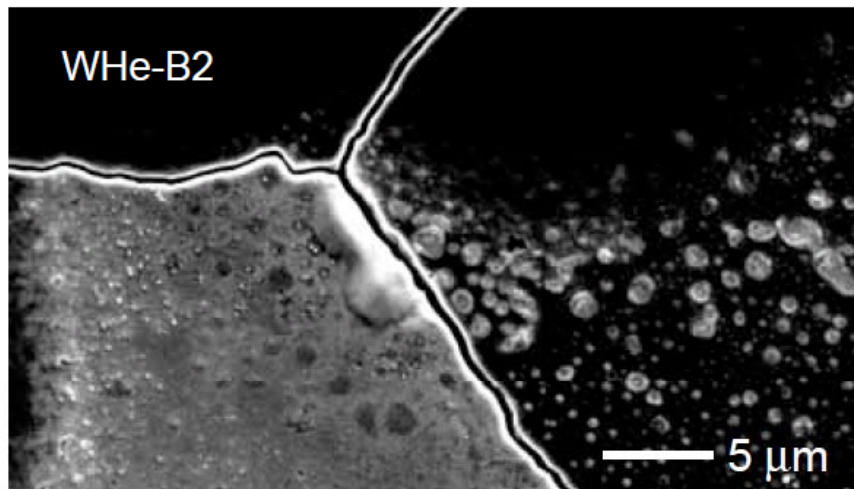


Fig. 3. W surface cracking on WHe-B2 after 10 shots with $\sim 0.5 \text{ MJ/m}^2$ per shot.

D. Nishijima, Y. Kikuchi et al., 9th Int. Conf. on Tritium Science & Technology, Nara, Japan Oct. 24-29, 2010, accepted for publication in Fusion Science and Technology.

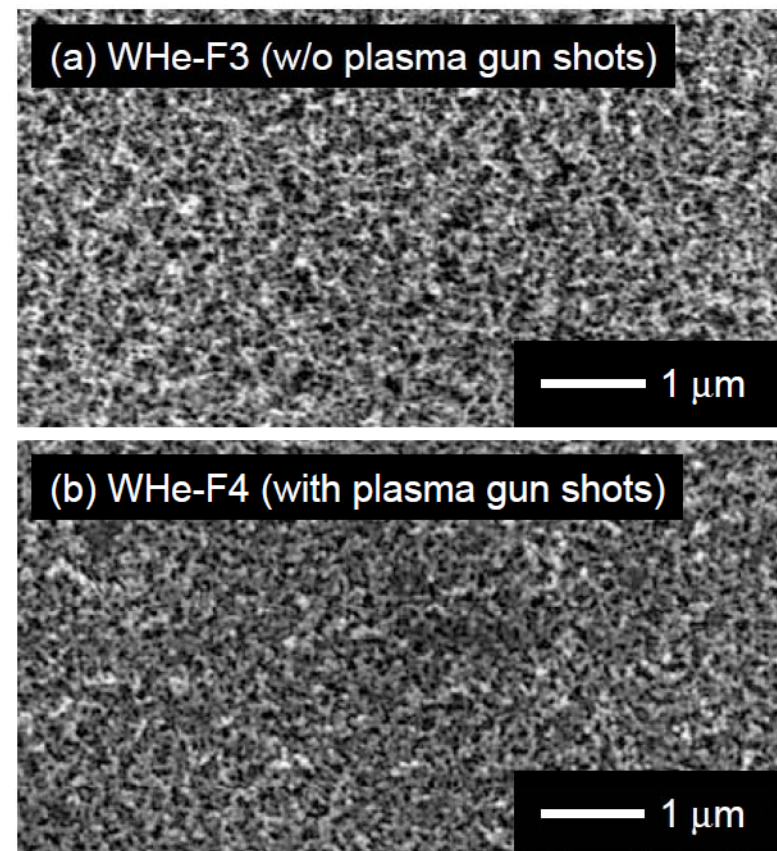
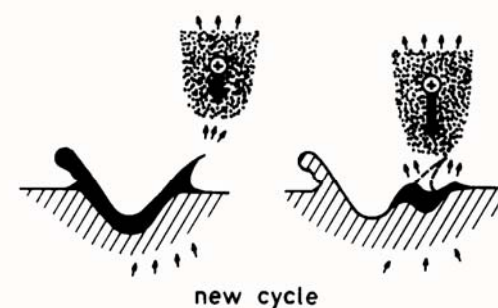
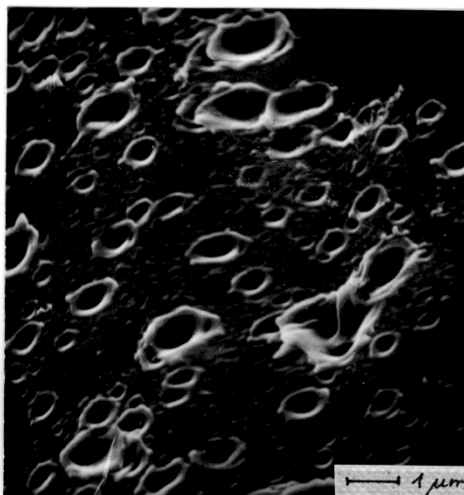
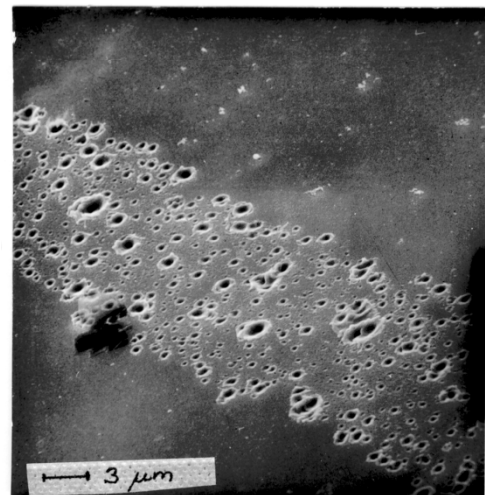
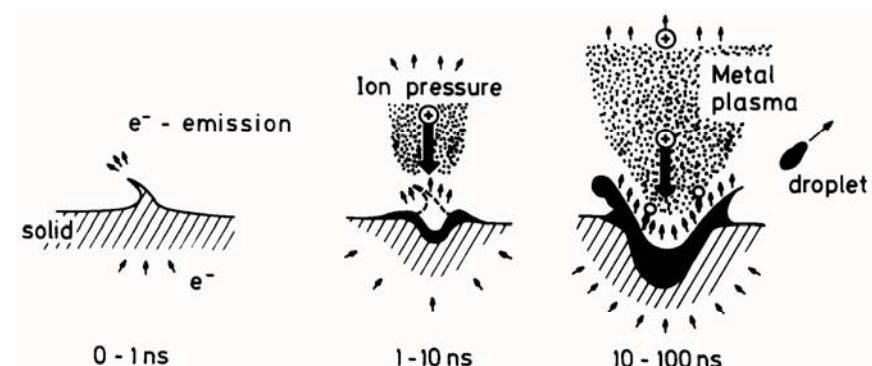
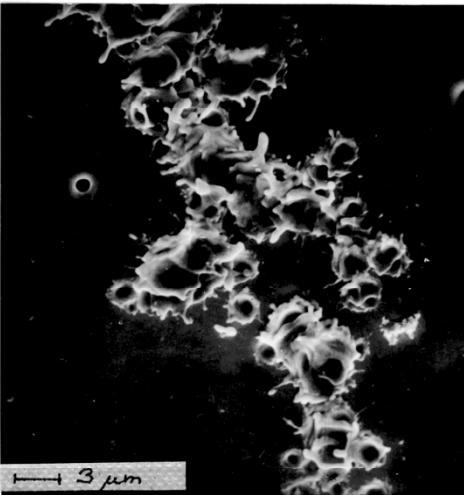
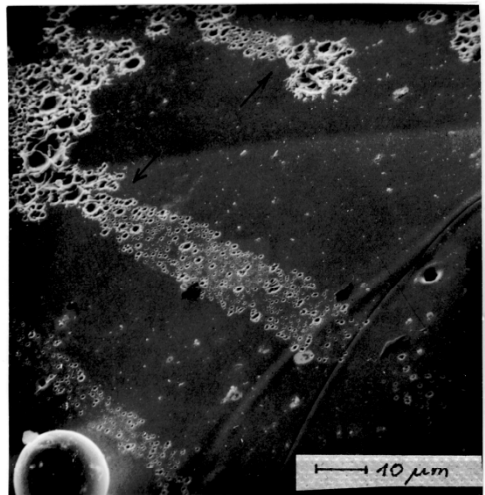


Fig. 4. SEM images of fuzzy W surfaces ($L_{\text{fuzz}} \sim 3 \mu\text{m}$). (a) WHe-F3: without plasma gun shots. (b) WHe-F4: after 10 plasma gun shots with $\sim 0.7 \text{ MJ/m}^2$ per shot.

Arcing on Metal Surfaces



B. Juttner: Plasmaphys. **19** (1979) 25

Unfavorable Property : Unipolar Arc

Does nanostructure tend to trigger unipolar arc on the W surface ?

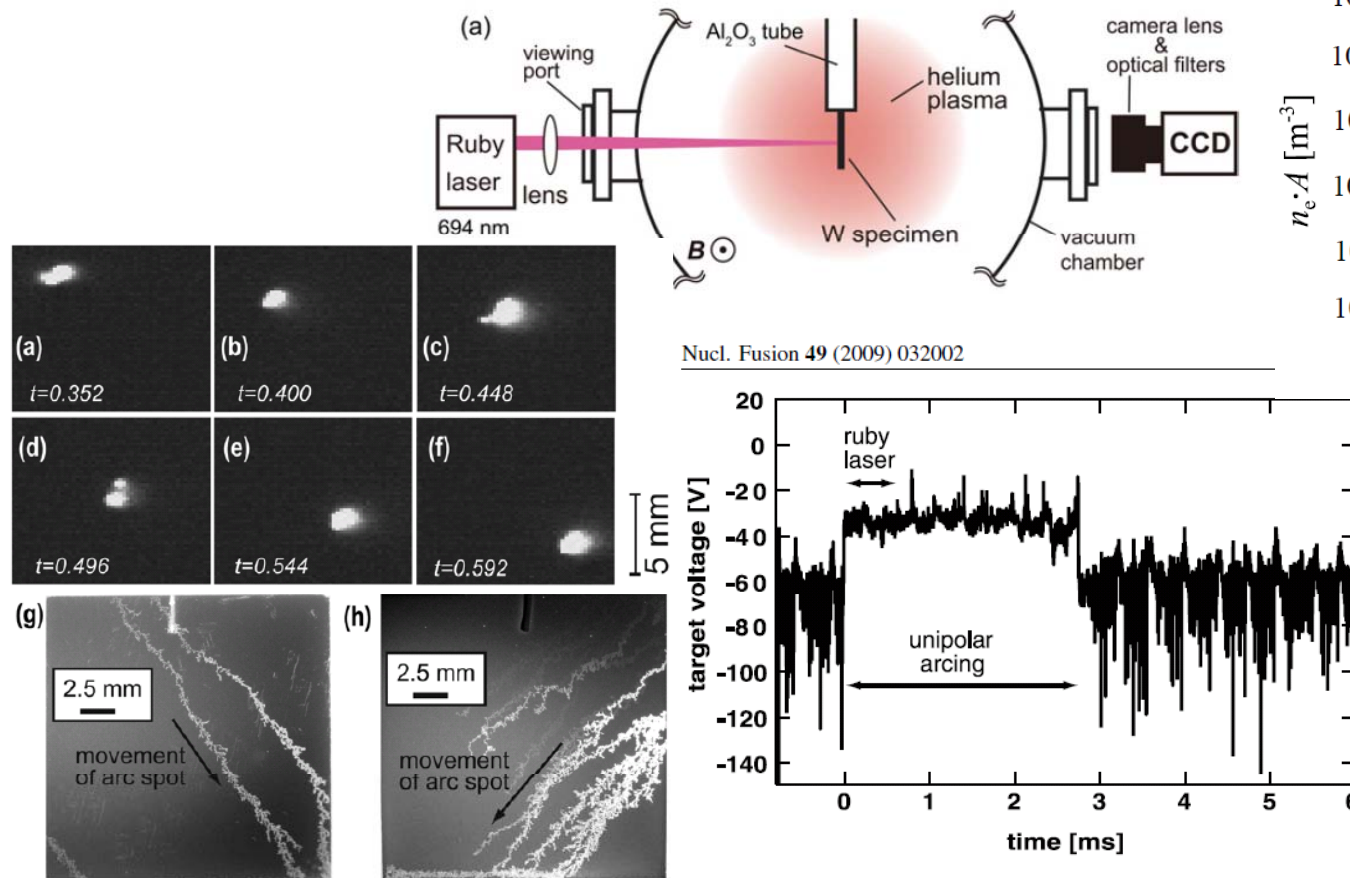
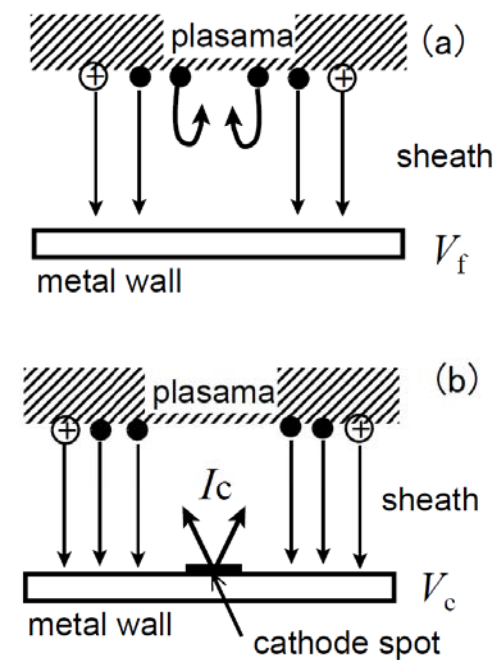
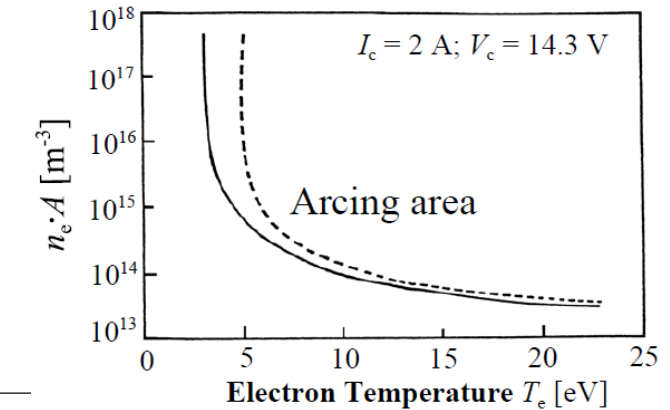
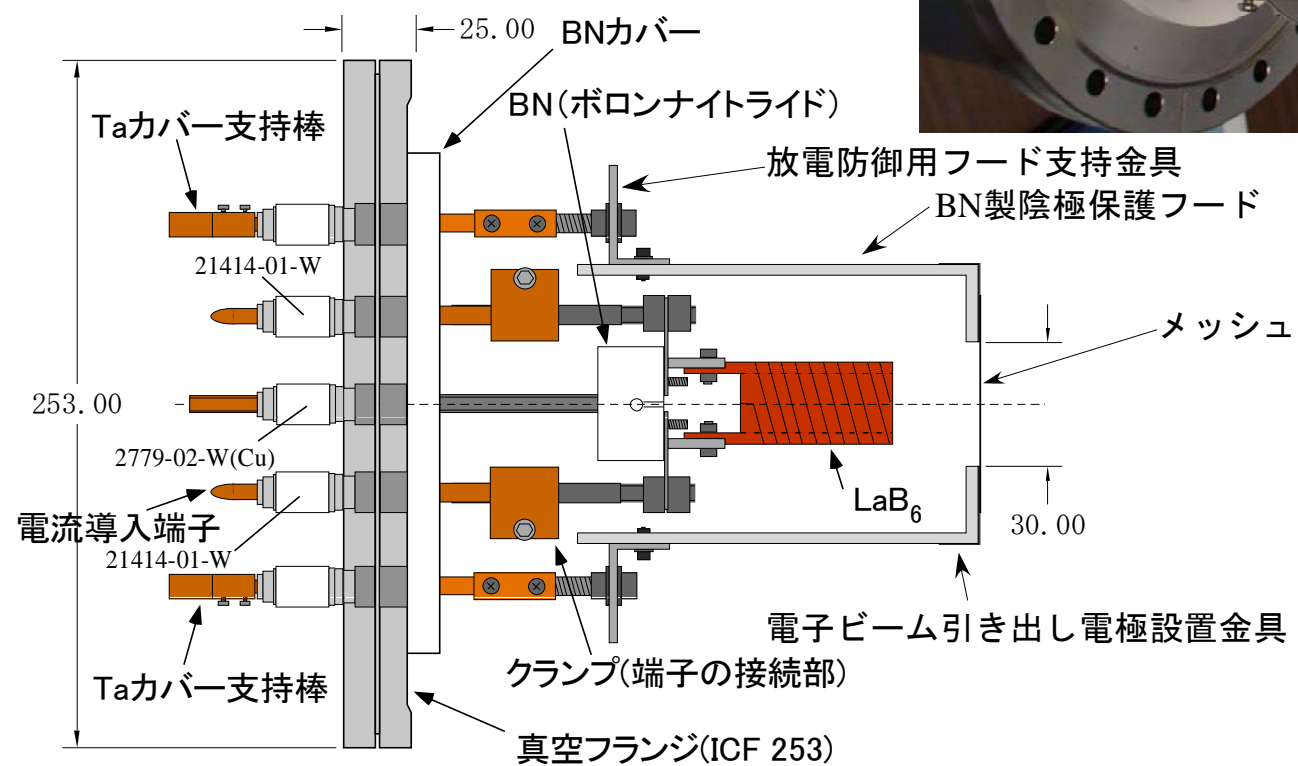
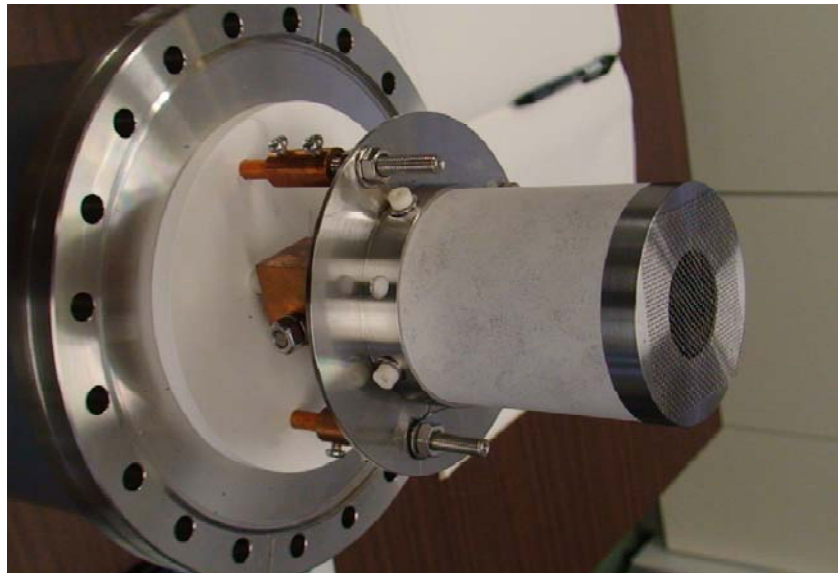
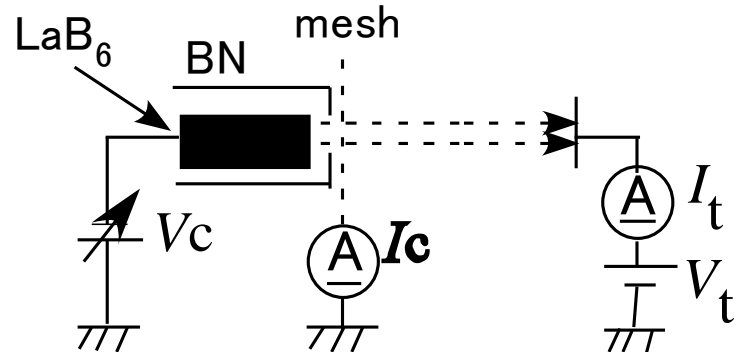


Figure 4. (a)–(f) show the temporal evolution of the emission W_I ($\lambda = 429.5$ nm) at every 48 μ s from a cathode spot running on the electrode, for the configuration for case (i). (g) and (h) are pictures of the back (the non-laser-irradiated side) of the electrode surface after the experiments with configurations (i) and (ii), respectively.

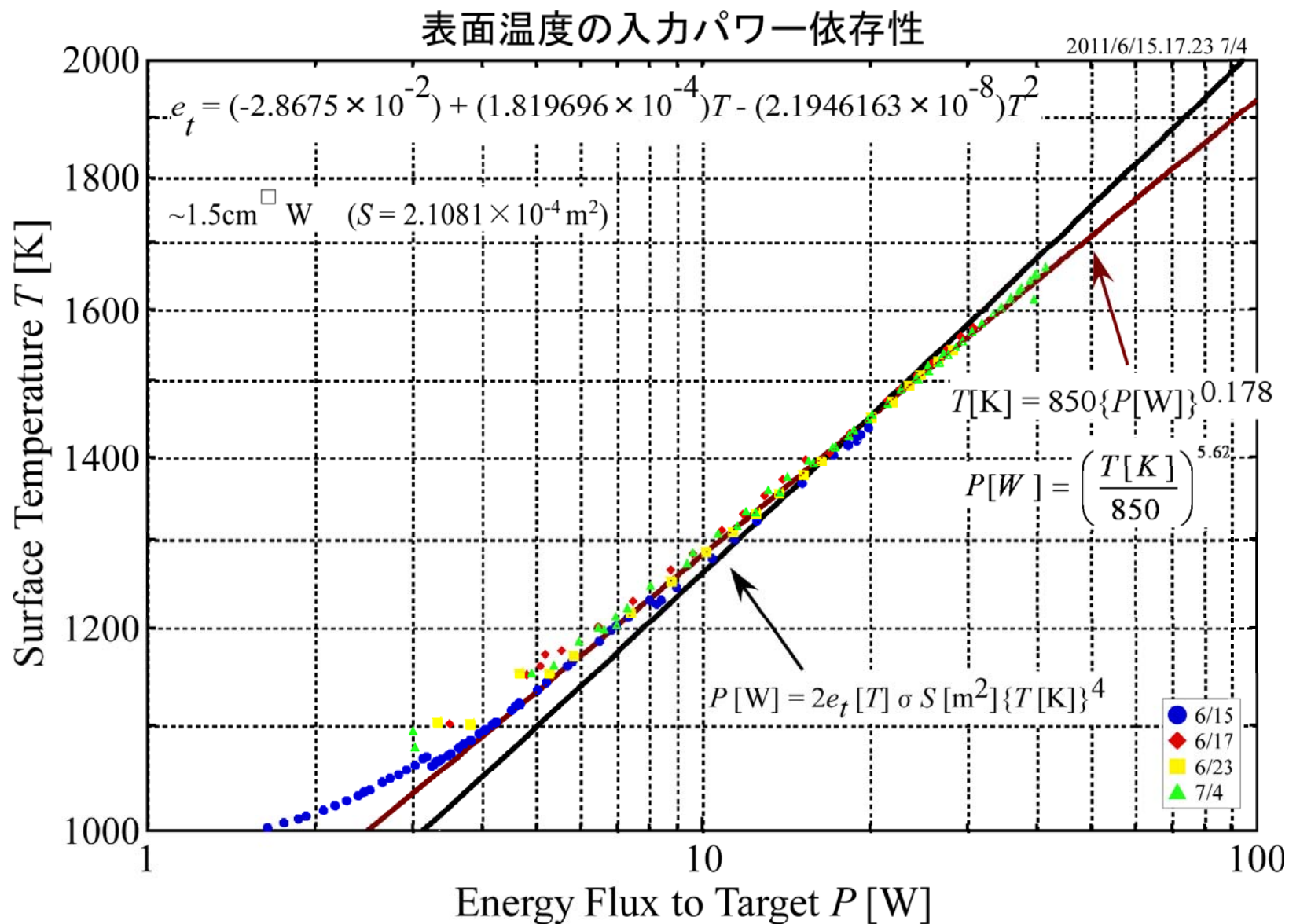
Figure 3. The temporal evolution of the electrode potential. The potential increase in response to the laser pulse irradiation indicates the initiation of unipolar arcing. The potential increase continues for approximately 2.8 ms, which is much longer than the laser pulse width (~ 0.6 ms), indicating free-running unipolar arcing.



タンクステンからの熱放射特性1



タンクステンからの熱放射特性2



W表面特性に関するまとめ

- (1) プラズマアニーリングによりナノ構造を消失させ表面修復させることができる。しかし修復面直下に微少バブル列が残る。これらはKrasheninnikovによるWの粘性とバブル形成に基づく成長モデルと矛盾しない。
- (2) ナノ構造形成過程においては、W表面の冷却がおきることを熱電対による直接計測で実証。これは
全放射率の上昇と
2次電子放出抑制に伴う浮遊電位の低下がシースの熱伝達係数を引き下げることの両方に起因する。ELM襲来に効果的ではないか。
- (3) **ナノ構造形成**により、**物理スパッタリング**が著しく抑えられる。極小の時の表面モルフォロジーは成長直後のそれと少し異なるが理由はわからない。
- (4) ナノ構造は過渡熱負荷に伴うクラッキングに耐性があることを紹介。
- (5) アーキングを誘発しやすい性質は、ナノ構造Wが自己防衛的核融合炉壁とする最大の難点。抑制する手立てはないか？
- (6) 損傷を受けていないW表面からの熱放射特性の全貌が明らかになりつつある。これを損傷Wに拡張することが課題。